0026-895X/00/5901-96–103$3.00
MOLECULAR PHARMACOLOGY
Copyright © 2000 The American Society for Pharmacology and Experimental Therapeutics
Mol Pharmacol 59:96–103, 2000

Vol. 59, No. 1
111/875640
Printed in U.S.A.

DNA-Interactive Anticancer Aza-Anthrapyrazoles: Biophysical and Biochemical Studies Relevant to the Mechanism of Action

C. SISSI, S. MORO, S. RICHTER, B. GATTO, E. MENTA, S. SPINELLI, A. P. KRAPCHO, F. ZUNINO, and M. PALUMBO

Department of Pharmaceutical Sciences, University of Padova, Padova, Italy (C.S., S.M., S.R., B.G., M.P.); Novuspharma, Monza, Italy (E.M., S.S.); Chemistry Department, University of Vermont, Burlington, Vermont (A.P.K.); and Istituto Nazionale Tumori, Oncologia Sperimentale B, Milan, Italy (F.Z.)

Received February 28, 2000; accepted October 2, 2000

This paper is available online at http://molpharm.aspetjournals.org

ABSTRACT

The physicochemical and DNA-binding properties of anticancer 9-aza-anthrapyrazoles (9-aza-APs) were investigated and compared with the carbocyclic analogs losoxantrone (LX) and mitoxantrone (MX). Unlike their carbocyclic counterparts, the tested 9-aza-APs do not undergo self-aggregation phenomena. The pyridine nitrogen at position 9, missing in the carbocyclic derivatives, is involved in protonation equilibria at physiological pH. In addition, 9-aza-APs are electrochemically reduced at a potential intermediate between LX and MX. These data fully agree with quantum mechanical calculations. Binding to nucleic acids was examined by spectroscopic, chiroptical, and DNase I footprinting techniques as a function of ionic strength and base composition. The 9-aza-APs exhibit prominent affinity for DNA, with an important electrostatic contribution to the binding free energy. A very remarkable sequence preference pattern dramatically favors GC steps in double-helical DNA, whereas the carbocyclic reference compounds show a substantially lower selectivity for GC. A common DNA complexation geometry, considerably differing from that of MX, characterizes all anthrapyrazoles. Hence, bioisosteric substitution and ring-hydroxy deletion play an important role in defining the physicochemical properties and in modulating the affinity of anthrapyrazoles for the nucleic acid, the geometry of the intercalation complex, and the sequence specific contacts along the DNA chain. Drug stimulation of topoisomerase II-mediated DNA cleavage is remarkably attenuated in the aza-bioisosteric derivatives, suggesting that other non-enzyme-mediated cytotoxic mechanism(s), possibly connected with free radical production, are responsible for efficient cell killing. The biophysical and biochemical properties exhibited by 9-aza-APs contribute to clarifying the peculiar pharmacological profile of this family of compounds.

Anthracenedione-based drugs are characterized by prominent anticancer properties and are widely used in clinical practice (Hortobagyi, 1997; Thomas and Archimbaud, 1997; Wiseman and Spencer, 1997; Arcamone, 1998). Their mechanism of action has been principally correlated to their ability to stimulate DNA cleavage mediated by the enzyme topoisomerase II (Malonne and Atassi, 1997). Nonetheless, recent studies have shown that the telomeric G-quadruplex structure, which interferes with the function of telomerase, can be efficiently targeted by anthraquinones (Perry et al., 1998, 1999). In addition, it is well known that the redox cycling of the anthracenedione ring system may generate reactive radical species that are believed to be responsible for a number of toxic effects, including cardiac toxicity (Frishman et al., 1997; Giantris et al., 1998).

With the aim of developing new effective drugs, the aza-anthracenedione family was recently obtained and tested (Krapcho et al., 1994; Hazlehurst et al., 1995a,b; Krapcho et al., 1995; De Isabella et al., 1995; Sissi et al., 1996; De Isabella et al., 1997; Sissi et al., 1999). These drugs are structurally related to the anthracenedione mitoxantrone (MX) but contain a heterocyclic, rather than a carbocyclic, chromophore. The positioning of the nitrogen atom within the heterocyclic backbone plays a critical role for activity (Krapcho et al., 1994, 1995). Indeed, substitution of the pyridine for the dihydroxyphenylene ring in the planar chromophore of MX affects the cytotoxic activity and the ability to stimulate topoisomerase II-mediated DNA damage in intact cells and with simian virus 40 DNA in vitro. The 2-aza derivatives are substantially more potent than the 1-aza or the 2,3 di-aza congeners against L1210 cells in vitro. The same trend is confirmed when the drugs are tested in vivo. In fact, the 2-aza-anthracenediones showed marked antitumor activity, in some cases curative, whereas the 1-aza-anthracenediones were essentially inactive.

Chromophore modification of the anthracenediones related to MX led to the anthrapyrazole class of compounds (Showalter et al., 1987), among which losoxantrone (LX) emerged

ABBREVIATIONS: MX, mitoxantrone; LX, losoxantrone; 9-aza-AP, 9-aza-anthrapyrazole; BBR 3438, (2-[2-[(2-hydroxyethyl)amino]ethyl]-5-[[2-methylamino)ethyl]amino] indazolo[4,3-gh]isoquinolin-6(2H)-one dihydrochloride salt); BBR 3576, (5-[[2-(dimethylamino)ethyl]amino]-2-[2-[(2-hydroxyethyl)amino]ethyl]indazolo[4,3-gh]isoquinolin-6(2H)-one dihydrochloride salt); LUMO, lowest unoccupied molecular orbital; SV, simian virus.

as the most promising clinical candidate. This compound has demonstrated good clinical efficacy in the treatment of breast cancer (Talbot et al., 1991) but cardiac toxicity was still observed during the clinical trials (Walsh et al., 1995).

Because in the anthracenedione series the nitrogen for carbon bioisosteric substitution retains antitumor activity and abolishes cardiotoxicity, it seemed to be of interest to synthesize and test novel aza-analogs of the anthrapyrazole ring structure. In particular, the 9-aza-derivatives (9-aza-APs) seemed to be very promising. (Krapcho and Menta, 1997; Krapcho et al., 1998). In vitro evaluation of 9-aza-APs demonstrated high cytotoxic potency and the ability of overcoming multidrug resistance induced in a doxorubicin-resistant cell line. In addition, 9-aza-APs were highly effective in vivo against both systemic P388 murine leukemia and MX-1 human mammary carcinoma transplanted in nude mice. On the basis of their efficacy profile in additional experimental tumors and lack of cardiotoxicity in preclinical models (Krapcho and Menta, 1997), two derivatives, BBR 3438 and BBR 3576 (Fig. 1), have surfaced as potential clinical candidates. They can be considered as bioisosteric analogs of the experimental anthrapyrazole LX. To better understand the factors influencing pharmacological activity in the 9-APs family, in this article we will evaluate a number of physicochemical properties of the new compounds, including self-aggregation, redox cycling, hydrophobicity, and energetics, along with affinity and specificity for DNA. In addition, topoisomerase-mediated stimulation of DNA cleavage will be examined. For comparison, two carbocyclic analogs MX and LX (Fig. 1) will be also investigated.

Experimental Procedures

Materials. BBR 3438 (2-[2-[(2-hydroxyethyl)amino]ethyl]-5-[[2-methylamino)ethyl]amino] indazolo[4,3-gh]isoquinolin-6(2H)-one dihydrochloride salt) and BBR 3576 (5-[[2-(dimethylamino)ethyl]-amino]-2-[2-[(2-hydroxyethyl)amino]ethyl]indazolo[4,3-gh]isoquinolin-6(2H)-one dihydrochloride salt) were synthesized as described previously (Krapcho et al., 1998). Losoxantrone was synthesized according to the published procedure (Beylin et al., 1989). Mitoxantrone was a generous gift of Lederle (Catania, Italy). Stock solutions (1 mg/ml) of test compounds were prepared in deionized water and diluted to the appropriate concentration in the working buffer before use.

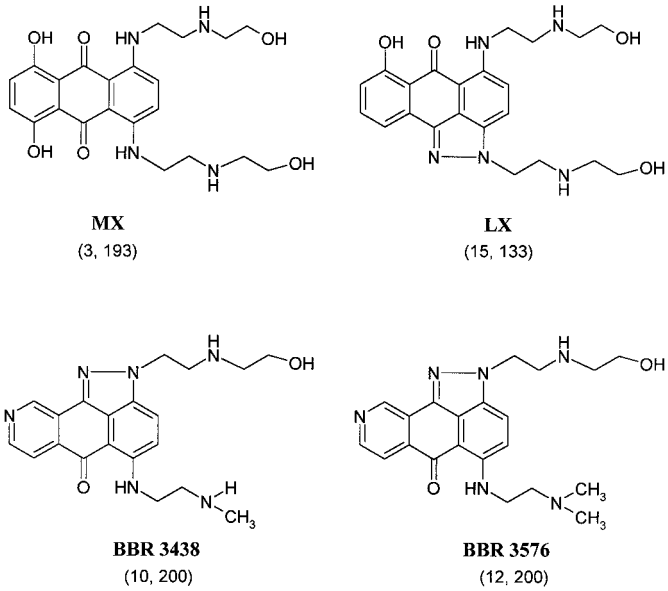

Fig. 1. Chemical structure of the test compounds and activity against murine leukemia L1210 (in brackets: optimal dose in milligrams per kilogram per day and percentage increase in lifespan).

The three natural DNAs from calf thymus (ctDNA, highly polymerized sodium salt), *Clostridium perfringens* (*Cp* DNA), and *Micrococcus lysodeikticus* (*Ml* DNA), together with the double-stranded alternating polynucleotides poly(dG-dC) and poly(dA-dT), were purchased from Pharmacia (Milan, Italy) or Sigma (St. Louis, MO). Their concentrations were determined applying the molar extinction coefficients given in the literature (Grant et al., 1968; Wells et al., 1970).

γ-ATP labeled with ^{32}P was obtained from Amersham Pharmacia Biotech (3000 Ci/mmol; Piscataway, NJ). Alkaline phosphatase and T4 polynucleotide kinase were purchased from Boehringer Mannheim (Mannheim, Germany) and used according to the supplier's recommended protocol in the activity buffer provided.

All other chemicals were analytical grade reagents, and all solutions were prepared using doubly deionized, Millipore-filtered water.

DNA Binding Studies. Fluorometric measurements were performed with a Perkin-Elmer LS30 fluorometer, equipped with a Haake F3-C thermostat. Additional spectrophotometric titrations were performed with a Perkin-Elmer Lambda 12 apparatus. Titrations were carried out at 25°C in ETN (1 mM EDTA, 10 mM Tris·HCl, pH 7.0, and NaCl to obtain the desired ionic strength). Binding was followed by addition of increasing amounts of DNA to a freshly prepared drug solution. To avoid large systematic inaccuracies caused by experimental errors, the range of bound drug fractions used for calculations was 0.15 to 0.85. Data were evaluated according to the equation of McGhee and Von Hippel (1974) for noncooperative ligand-lattice interactions:

$$r/m = K_1(1 - nr)^n/[1 - (n - 1)r]^{n-1}$$

where r is the molar ratio of bound ligand to DNA, m is the free ligand concentration, K_i is the intrinsic binding constant, and n is the exclusion parameter.

Cyclic Voltametry. Cyclic voltametry measurements were carried out under a nitrogen flux, at 25°C in a 0.1 M phosphate buffer, pH 7.0. A three-electrode system was used with a reference saturated calomel electrode and a platinum wire counter electrode; the working electrode was a glassy carbon electrode.

Potentiometric Titrations. Potentiometric and spectroscopic titrations were performed in 50 mM NaCl to follow the protonation state of the test compounds. Drugs were dissolved in saline solution at concentrations in the range 10^{-3} to 10^{-5} M. Changes of the optical properties were recorded with a Perkin-Elmer Lambda 12 apparatus upon addition of known amounts of standardized NaOH or HCl solutions, and the pH measured with a Metrohm 713 pH Meter.

5′-End-Labeled DNA Fragments. Two 5′-end-labeled DNA fragments were prepared by PCR. Briefly, one synthetic primer was labeled with [γ-^{32}P]ATP and T4 polynucleotide kinase in the appropriate buffer. After phenol-chloroform extraction and ethanol precipitation, it was used to amplify the selected plasmid fragment. The uniquely 5′-end-labeled DNA fragment was then purified on a 8% polyacrylamide gel under native conditions in TBE buffer (89 mM Tris base, 89 mM boric acid, and 2 mM EDTA). After autoradiography, the 5′-end-labeled DNA was excised, crushed, and soaked in elution buffer (500 mM sodium acetate) overnight at 37°C. This suspension was filtered through a Millipore 0.22-μm filter and the DNA was precipitated with ethanol. After washing with 70% ethanol and vacuum drying of the precipitate, the labeled DNA was resuspended in 10 mM Tris adjusted to pH 7.0 containing 10 mM NaCl.

DNase I Footprinting. Experiments were performed essentially as described previously (Sissi et al., 1996). 5′-Labeled DNA (20,000 cpm) were mixed with unlabeled DNA (15 μM, final concentration)

and increasing concentrations of the test drugs in 8 μl of DNase I buffer (40 mM Tris HCl, pH 7.9, 10 mM NaCl, 6 mM $MgCl_2$, 0.1 mM $CaCl_2$). The mixture was incubated for 30 min at room temperature to allow equilibration of the binding reaction, then digestion was initiated by the addition of 2 μl of a DNase I solution (1.5 U/ml, final concentration). After 3 min, the reaction was stopped by adding 2 μl of carrier solution (0.3 M Na acetate, 1 mM EDTA, 50 μg/ml tRNA) and freeze-drying. Samples were lyophilized and resuspended in 5 μl of an 80% formamide solution containing tracking dyes. Samples were then heated at 90°C for 4 min and chilled in ice and loaded onto 8% denaturing polyacrylamide gel (19:1) in TBE buffer. Gels were transferred to Whatman 3 MM paper, dried under vacuum at 80°C and autoradiographed (Amersham Hyperfilm MP) at −70°C with an intensifying screen. Each resolved band was assigned to a particular bond within the DNA fragment by comparison of its position relative to sequencing standards generated by treatment of the DNA with formic acid followed by piperidine-induced cleavage at the modified bases (G+A) in DNA (Maxam and Gilbert, 1977).

Topoisomerase II Assay. In a total volume of 20 μl, 50 ng of 5′ ^{32}P-labeled DNA (SV 40 fragment 2533–2757) were incubated with 1.2 U of topoisomerase II (Topogen, Columbus, OH) in the absence or presence of increasing drug concentrations in 50 mM Tris·HCl, pH 8.0, 120 mM KCl, 10 mM $MgCl_2$, 0.5 mM ATP, 0.5 mM DTT, and 30 μg/ml BSA. The mixture was incubated for 20 min at 37°C. Reaction was stopped by adding 5 μl of stop mixture (5% SDS, 2.5 mg/ml protein kinase, 5 ng cold DNA) and incubating for 45 min at 50°C. The reaction products were precipitated and resuspended in 5 μl of an 80% formamide solution containing tracking dyes. Samples were then heated at 90°C for 4 min and chilled in ice and loaded onto 8% denaturing polyacrylamide gel (19:1) in TBE (89 mM TRIS base, 89 mM boric acid, 2 mM Na_2EDTA). Gels were transferred to Whatman 3 MM paper, dried under vacuum at 80°C, and autoradiographed (Amersham Hyperfilm MP) at −70°C with an intensifying screen.

Chiroptical Studies. Circular dichroism spectra were recorded on a Jasco 710 spectropolarimeter. Quartz cells having a 10 mm path length were used. Four to eight scans were accumulated for each measurement.

Computational Methodologies. Calculations were performed on a Silicon Graphics O2 R10000 workstation and on an NT workstation (PIII-450 MHz dual processor). Mitoxantrone and aza-anthrapyrazole models were constructed using the "Molecule Builder" module of Molecular Operating Environment (MOE 1999.05; Chemical Computing Group Inc., Quebec, Canada). Conformational analysis of all derivatives was performed on all rotatable bonds of both side chains using a random search procedure implemented in MOE. These structures were minimized using MMFF94 force field (Halgren, 1996c; Halgren and Nachbar, 1996) until the *rms* value of Truncated Newton method (TN) was < 0.001 kcal/mol/Å. The optimized geometries of all structures were fully minimized using RHF/AM1//RHF/3–21G(*) *ab initio* level of Spartan Pro v.1.0.1.(Halgren, 1996b) RHF/AM1-SM5.4 method has been used for treatment of molecules in water (Halgren, 1996a). Atomic charges were calculated by fitting to electrostatic potential maps.

LogP values (the log of the *n*-octanol/water partition coefficient), a hydrophobicity indicator, were empirically calculated using the atom fragment method implemented in the "QuaSAR-Descriptor" module of MOE.

Results

Physicochemical Properties of 9-Aza-Anthrapyrazoles

Spectroscopic Studies. Both aza-anthrapyrazoles show two absorption bands in the visible range, located at 471 and 493 nm in ETN buffer, pH 7.0. The dependence of the absorbance upon drug concentration was investigated to evaluate the presence of self-aggregation equilibria that are prominent for MX (Lown et al., 1985). LX was also examined for comparison. Although for the 9-aza-APs a linear plot of absorbance versus concentration was observed in the working concentration range (up to 2×10^{-5} M), remarkable deviations from linearity were found for LX (not shown).

Redox Potentials. It is well known that anthraquinone derivatives like mitoxantrone and anthracyclines undergo redox processes, with the production of cell-damaging free radicals. This is especially true for aza-anthracenediones, which seem to be operating through this mechanism to a large extent (De Isabella et al., 1995). The redox properties of test compounds were evaluated by cyclic voltametry experiments. A typical voltamogram for BBR 3576 and MX is shown in Fig. 2, and the results are summarized in Table 1.

The first reduction process, corresponding to reduction of the imino-quinone system, occurs for the aza derivatives at remarkably lower potential compared with the carbocyclic analog LX (−0.8 versus −1.1 V). As expected, introduction of the pyrazole ring renders reduction more difficult by lowering the reduction potential by 0.3 to 0.4 V with respect to the anthraquinone congeners. The lack of OH groups may additionally affect the half-wave potential.

Acidity Constants. The spectroscopic pKa values were obtained from the absorbance changes exhibited by 9-aza-APs as a function of pH. The possible sites of protonation are the two side-chain nitrogens, the 9-aza-nitrogen, and the pyrazole nitrogens. The pK_a values obtained from potentiometric and spectrophotometric titration experiments are summarized in Table 2. The pK_1 and pK_2 values refer to proton release occurring at the pyrazole and 9-aza nitrogen, respectively. Clearly, the side-chain substituents do not influence the above values to an appreciable extent. On the contrary, a difference of 0.4 p*K* units is observed when considering the pK3 value. This value is obtained as the average of the protonation states of the two side-chain nitrogens. In this case, the difference reflects the different acidity of the side-chain protonated secondary and tertiary amine of BBR 3438 and BBR 3576, the other side chain being identical for the two compounds. Apparently, the tertiary amine is less basic than the secondary amine in aqueous media.

Molecular Modeling. A molecular modeling study has been carried out to better describe the crucial differences concerning the chemical and pharmacological behavior of anthrapyrazole and aza-anthrapyrazole derivatives. We have analyzed, in detail, biased mitoxantrone (MX), BBR 3576,

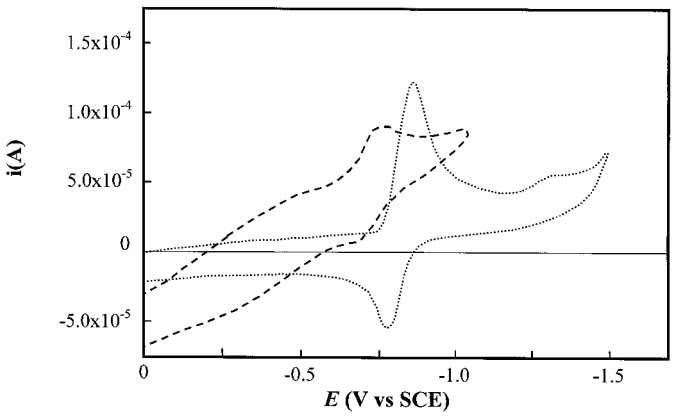

Fig. 2. Calculated energies for the protonation of basic nitrogen sites in BBR 3576.

and the carbocyclic analog LX. From the structural point of view MX, LX, and BBR 3576 present comparable steric requirements, as clearly shown, analyzing the corresponding values of molecular surface and volume (see Table 3). Indeed, the replacement of one 2-[(2-hydroxyethyl)amino]ethyl side-chain of LX with a 2-(dimethylamino)ethyl substituent reduces both molecular surface and volume of BBR 3576. Comparing the logP values, MX shows the highest hydrophilicity (logP, −0.54) whereas BBR 3576 and LX show almost the same value (logP, −0.11 and 0.06, respectively). On the other hand, when we compare the contribution of the solvation, BBR 3576 seems to be less hydrated than LX ($\Delta H_{hydration}$ = −17.4 and −22.5 kcal/mol, respectively); consequently, BBR 3576 could exhibit higher affinity to hydrophobic environments.

Another interesting consideration concerns the protonation of the aza-anthrapyrazole system. As mentioned above, it was experimentally possible to identify three main pH transitions. AM1 and AM1-SM5.4 calculations have been used to investigate the basicities of the aza-anthrapyrazole nitrogen atoms of BBR 3576 in the gas phase and to account for changes in basicities from the gas phase to water. As shown in Fig. 3, in full agreement with the experimental titration experiments, at pK_1 we observe the N-protonation of the pyrazole system, at pK_2 the N-protonation of the pyridine moiety, and, at pK_3, probably the sum of the protonation of the nitrogen atoms of the two side-chains.

The energy of the lowest unoccupied molecular orbital (LUMO) is included in Table 1. It is lowest for MX, intermediate for the 9-aza-AP, and highest for LX.

DNA-Binding of 9-Aza-Anthrapyrazoles

Binding Affinity. The test 9-aza-APs give an intense fluorescence emission, allowing us to work at drug concentrations as low as 0.1 μM. Hence, we used this technique to evaluate the DNA binding parameters and to investigate the effects of ionic strength and base composition on complex formation. Addition of ctDNA to test compounds induces a dramatic drop in the fluorescence quantum yield (Fig. 4), which allows the calculation of free and DNA-bound drug. Analysis of the binding data gave the thermodynamic parameters reported in Table 4. Both 9-aza-APs bind DNA efficiently. The exclusion parameter, n, is always close to 2 base pair, which is consistent with an intercalation process, further confirmed by gel electrophoresis unwinding experiments using plasmid DNA (not shown). Clearly, methylation of the side-chain of the aza-anthrapyrazole BBR 3438 to give BBR 3576 does not affect the DNA binding properties to an appreciable extent, whereas the introduction of the 9-aza group produces a 2-fold increase in affinity for the nucleic acid, giving K_i values even greater than MX. It is interesting to note that this enhanced affinity is observed in the absence of

TABLE 1
Redox properties of the test compounds measured by cyclic voltametry in 0.1 M phosphate buffer, pH 7.0, 25°C. LUMO energies are reported for comparison.

Compound	$E_{1/2}$(V)[a]	LUMO (eV)[b]
BBR 3576	−0.83 ± 0.03	−1.13
BBR 3438	−0.85 ± 0.03	
LX	−1.12 ± 0.03	−1.09
MX	−0.76 ± 0.03	−1.29

[a] Half-wave reduction potential.
[b] Energy of the lowest unoccupied molecular orbital.

TABLE 2
Acidity constants of the test compounds measured by spectrophotometric and potentiometric titrations in 50 mM NaCl, 25°C

Compound	pK_1	pK_2	pK_3
BBR 3576	2.81 ± 0.03	6.82 ± 0.03	8.06 ± 0.03
BBR 3438	2.81 ± 0.03	6.80 ± 0.03	8.49 ± 0.03

TABLE 3
Calculated chemical-physical properties of MX, LX, and BBR 3576

	MX	LX	BBR 3576
Surface (Å^2)	500.54	493.01	468.05
Volume (Å^3)	491.60	477.91	453.64
Dipole (debye)	3.002	4.806	6.225
Log P	−0.54	−0.06	−0.11
ΔH_{hydra} (kcal/mol)	−23.037	−22.559	−17.424

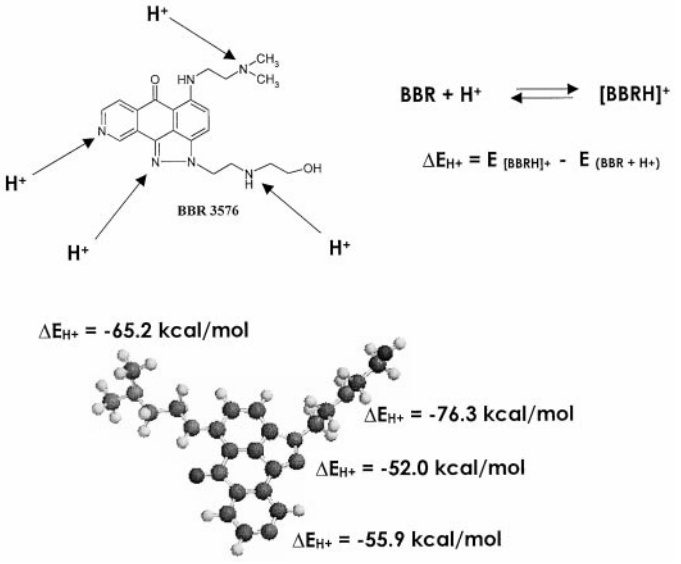

Fig. 3. Cyclic voltametry curves for MX and BBR3438 in 0.1 M phosphate buffer, pH 7.0, at 25°C. Scan rate, 200 mV/s.

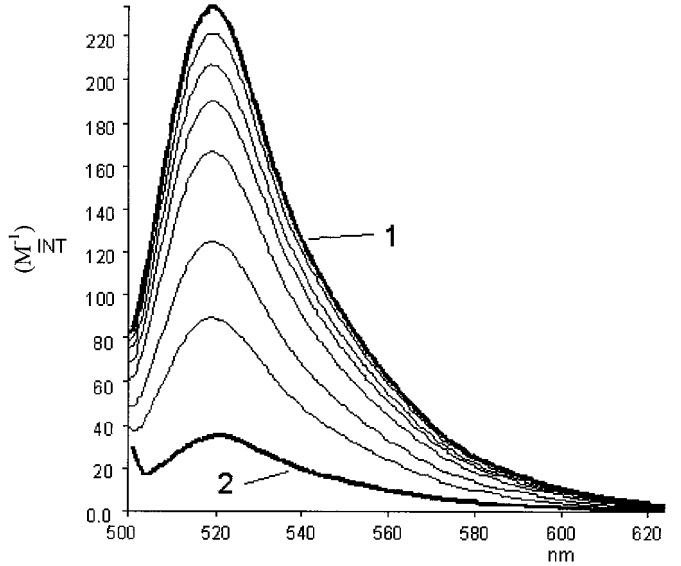

Fig. 4. Fluorometric titration of BBR 3438 (1 μM) upon addition of increasing amounts of DNA (0–1 mM). Excitation is performed at 410 nm. Curve 1, free drug; curve 2, fully bound drug.

hydroxy substituents in the aromatic ring system. It is in fact known that DNA affinity is substantially lowered upon ring-hydroxy deletion in MX to yield Ametantrone (Lown et al., 1985, Denny and Wakelin, 1990).

As expected from the charged nature of aza-anthrapyrazoles, increasing salt concentration leads to a drop in the binding constant K_i. This confirms the participation of the protonated side-chain substituents in stabilizing the drug-DNA complex. Because both drugs show a linear relationship of log K_i versus log (ionic strength), using the polyelectrolyte theory adapted to nucleic acids (Record et al., 1978), it is possible to evaluate the number of ionic contacts formed with DNA per molecule of bound 9-aza-AP (Table 5). In both cases, this value is close to 2.5. It accounts for the fact that, at neutral pH, in addition to both side-chain nitrogens, also the bioisosteric nitrogen at position 9 is partially protonated (see potentiometric titration experiments) and can contribute electrostatically to DNA binding. From the above value it can be estimated that roughly 50% of the 9-aza-anthrapyrazole molecules bind as doubly charged molecules and the remaining 50% as triply charged molecules. As predictable from the pK_a values reported in Table 2, this is independent of the level of methylation of the amine group in the side chain of the aza-anthrapyrazole.

Besides the number of charged interactions, it is possible to calculate the binding free energy corrected for the electrostatic contributions (Record et al., 1978), as shown in Table 5. A comparison of the above values with the free energy changes observed at physiological ionic strength indicates that ≈25% of the total free energy is caused by electrostatic interactions. Hence, notwithstanding the highly charged nature of 9-aza-APs, the large majority of the interaction energy comes from noncharged contacts. The figures relative to MX indicate that this anthracenedione binds more efficiently by nonelectrostatic interactions.

Sequence Specificity. Modulation of drug location along the polynucleotide chain can be relevant from a pharmacological point of view. Hence, we examined the sequence specificity of the test drugs using both spectrophotometric and DNase I footprinting techniques.

Spectrophotometric Studies. The binding properties of the test drugs were evaluated using natural and synthetic DNAs having different base pair composition. The calculated DNA binding constants are reported in Fig. 5 as a function of DNA composition. The two test aza-anthrapyrazoles exhibit very similar trends, again confirming that methylation of the side-chain does not affect DNA recognition to an appreciable extent. A very strong preference for GC steps in the nucleic acid was observed, that linearly decreased reducing the GC content. Indeed, it was not possible to calculate the K_i values for the binding to poly(dA-dT) because of the exceedingly low affinity of 9-aza-APs for this particular DNA sequence. On the contrary, LX exhibits a less pronounced preference, which seems to reach a maximum at intermediate GC% composition. Finally, MX also exhibits GC preference, but this is substantially less marked compared with that shown by aza-anthrapyrazoles.

TABLE 4
Thermodynamic binding properties of the test compounds to ctDNA in ETN buffer at different ionic strength, pH 7.0, 25°C

Compound	Ionic strength (M)	$K_i \times 10^{-5}$ $(M^{-1})^a$
BBR 3576	0.15	11.45 ± 1.35
	0.25	3.57 ± 0.42
	0.50	0.80 ± 0.03
BBR 3438	0.15	12.36 ± 0.94
	0.25	3.57 ± 0.31
	0.50	0.86 ± 0.06
MX	0.15	9.14 ± 0.60
LX	0.15	5.95 ± 0.56

[a] Intrinsic binding constant.

DNase I Footprinting Studies. The comparison between the two aza-anthrapyrazoles and LX or MX in terms of drug distribution among DNA-binding sites of different sequence was carried out also by DNase I footprinting experiments.

Two DNA sequences were used: one (fragment 906-1064 from pBR 322) rich in GC/CG steps and one (fragment 2533–2757 from SV 40) having an intermediate GC content.

On the pBR 322 fragment, obtaining a clear footprint pattern was not easy. In fact, under our experimental conditions, little variations of drug concentration led from an unmodified enzyme-mediated DNA digestion to a totally suppressed cleavage pattern (not shown). This is in line with the above-reported high binding affinity of aza-anthrapyrazoles for GC sequences.

More informative experiments, fully confirming GC preference, were carried out on the SV 40 fragment. The location of main DNase I inhibition/stimulation of cleavage by aza-APs is shown in Fig. 6. Preferred protection clearly occurs at alternating GC(T) sites.

It is worth mentioning that, whereas 9-aza-APs and LX gave comparable results at the same concentrations, higher amounts of MX were required to obtain a significant modification in the DNase I cleavage pattern. This possibly reflects

TABLE 5
Electrostatic contribution to the thermodynamic binding properties of the test compounds to ctDNA in ETN buffer, pH 7.0, 25°C

Compound	m′[a]	$-\Delta G_0$[b]	$-\Delta G$[c]
		kJ/mol	
BBR 3576	2.60 ± 0.12	25.3 ± 1.0	34.6 ± 1.0
BBR 3438	2.49 ± 0.13	25.7 ± 0.9	34.8 ± 1.1
MX	1.95 ± 0.12	30.7 ± 1.1	33.8 ± 0.9

[a] Number of ionic interactions per bound drug.
[b] Nonelectrostatic free energy contribution to the binding process.
[c] Free energy of binding at physiological (0.15 M) NaCl concentration.

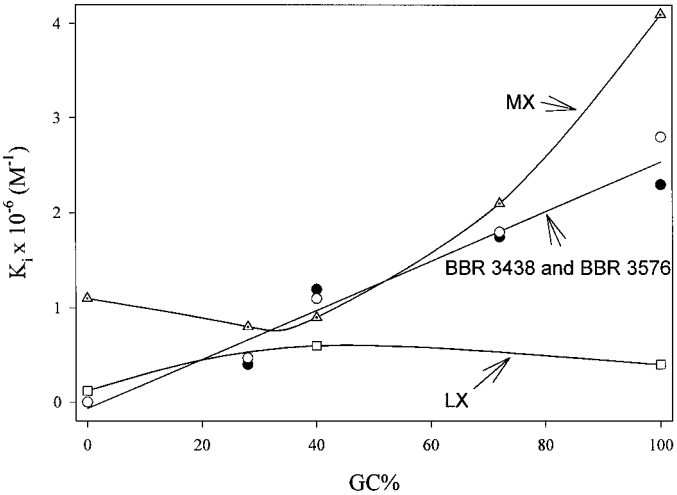

Fig. 5. Base sequence dependence of the intrinsic DNA binding constant (K_i) for the test drugs.

differences in residence times of different drugs onto the DNA template. It should be finally observed that the rather different specificity levels shown by spectroscopic studies when comparing 9-aza-APs with LX and MX seem to be attenuated in the DNase I cleavage experiments. Again, kinetic effects can be invoked to explain these findings.

Orientation of the Intercalated Chromophore. The test aza-anthrapyrazoles are not optically active, but when bound to DNA, an induced circular dichroism signal is observed in the visible region (drug absorption range). Because of the difficulties in interpreting the dichroic data using natural DNAs having a statistical display of all base-pair combinations, we examined the complexes formed with repeating synthetic polynucleotides. Hence, chiroptical studies were carried out with poly(dG-dC) as the nucleic acid; the complex with poly(dA-dT) could not be examined because of the very low affinity of this polynucleotide for 9-aza-Aps.

The spectra are reported in Fig. 7. All anthrapyrazole derivatives produce a negative induced CD that has a similar rotational strength. Instead, MX shows positive induced circular dichroism in the presence of alternating GC sequences.

Stimulation of Topoisomerase II-Mediated DNA Cleavage. The effects of the test drugs on topoisomerase II-mediated DNA cleavage were investigated on sequencing gels. Increasing amounts of MX, LX, and 9-aza-anthrapyrazoles (0.01–10 μM) caused bell-shaped levels of cleavage stimulation (not shown). At any given concentration, the extent of damage was affected by the nature of the drug, the ranking order being MX > LX > BBR 3438 ≈ BBR 3576. Common locations of the cleavage bands were shared by all derivatives. The principal sites of drug-stimulated cleavage in the SV 40 DNA fragment are shown in Fig. 6. They poorly overlap with the sites stimulated in the DNase I experiments presented in the same figure and generally include a cytosine at the position immediately preceding the cutting site (dots in the SV 40 sequence).

Discussion

The introduction of the bioisosteric nitrogen at position 9 of the anthrapyrazole ring structure and the concomitant removal of ring hydroxy substituents cause a number of physicochemical effects that are likely to be relevant in terms of biological activity.

The presence of the aza substituent abolishes self-aggregation phenomena occurring both for MX and LX. This is interesting, because self-aggregated species tend to precipitate from aqueous media causing obvious undesired consequences upon administration (Powis and Kovach, 1983). In addition, the aggregation phenomena subtract part of the drug from the pharmacologically relevant interactions. The reason for lack of aggregation probably rests in the protonation equilibria involving the pyridine nitrogen, which are significant at physiological pH. In fact, although the carbocyclic analogs can easily stack their neutral planar portion one onto the other with the charged side-chains oriented in opposite directions, the same process cannot occur in the case of the aza derivatives because of N-9 protonation. Indeed, in any direction one tries to stack two 9-aza-AP molecules, they will always experience unfavorable electrostatic repulsion, which will hardly allow any interaction between them.

The reduction potential is rendered less negative by aza substitution. Hence, the new compounds are reduced more easily than their carbocyclic counterparts. The extent of the increase in $E_{1/2}$ is about 0.3 V, which nearly corresponds to the effects found when anthracenediones are compared with aza-anthracenediones (De Isabella et al., 1995). These changes could be biologically relevant because a higher level of redox cycling could render 9-aza-APs more effective than LX in damaging cellular components. In agreement with this, preliminary data show that the 9-aza-anthrapyrazoles produced an increased extent of oxidative stress in a prostate carcinoma 3 cell line compared with the carbocyclic analog. Interestingly, the $E_{1/2}$ values seem to be well correlated to the theoretical LUMO energies (Table 1). This suggests that the effects caused by redox cycling could be anticipated from calculated LUMO energies. Hence, the latter may represent useful indicators for the electron-transfer processes occurring at the cellular level.

The binding of 9-aza-APs to double-stranded DNA is remarkably strengthened compared with LX and even MX. Interestingly, although a reduced affinity for DNA is found when the extra ring is introduced in the anthracenedione structure to give the anthrapyrazole (Hartley et al., 1988), the reverse is true in the case of the 9-aza bioisosteres. These findings possibly rest on two factors: first of all, the electrostatic contribution to the binding free energy at physiological conditions will be large for the highly charged aza-anthrapyrazole ($m' = 2.5$; see Table 5). This renders complex formation more efficient. Secondly, different intercalation geometry, with specific contacts involving the isosteric nitrogen, could be occurring. The latter case seems less

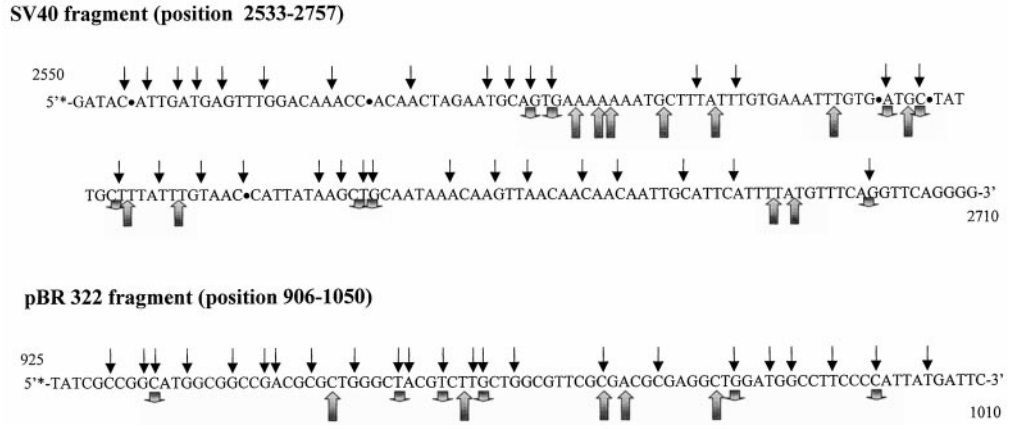

Fig. 6. Principal sites of protection and stimulation of cleavage observed for BBR 3438 and BBR 3576 in the SV 40 (sequence 2533–2757) and pBR322 (sequence 906-1050) DNA fragments. Dots in the SV 40 sequence represent preferred cleavage sites in the presence of Topoisomerase II. ↓, DNase I cleavage sites; short, down arrow with gradient fill, drug-inhibited cleavage sites; long, up arrow with gradient fill, drug-stimulated cleavage sites.

likely, because the circular dichroism measurements suggest a similar orientation of the intercalated chromophores for 9-aza-APs and LX. Moreover, the intercalation free energy, corrected for the electrostatic contribution (Table 5), is less negative than the energy found for MX, which again points to ionic effects having the main responsibility for increased affinity. It is worth recalling that the parent 2-aza-anthracenediones generally show a reduced DNA-binding constant compared with MX (De Isabella et al., 1995). In that case, ionic contributions are not strong enough ($m' \leq 2$) to counterbalance the less favorable energy change caused by intercalation of the N-substituted ring system.

9-Aza-APs exhibit a strong discrimination for GC versus AT base pairs, much more pronounced than the carbocyclic analogs. This effect is surely caused by the simultaneous presence of the 9-aza and pyrazole groups in the molecule. In fact, aza-anthracenediones showed a generally lower specificity for DNA binding (and topoisomerase poisoning) (Sissi et al., 1996), accepting a wider number of sequences compared with MX. In addition, LX itself seems to be less GC-specific than MX (Fig. 5). The origin(s) of increased base selectivity for the test drugs is related to very poor affinity for AT steps, rather than with increased affinity for GC (Fig. 5). The reason for this is not apparent at present.

LX and its aza-congeners exhibit almost identical induced rotational strength when bound to poly(dG-dC). Although compensations could occur from changes in direction of the transition moment of the two types of intercalated molecules and from lateral displacements from the helix axis (Lyng et al., 1991), it seems from the very similar dichroic response that the orientations of the anthrapyrazole and aza-anthrapyrazole chromophores are very similar in the intercalation pocket. MX behaves in the opposite way, inducing positive rotational strength when bound at GC steps. This points to substantial changes in chromophore orientation for the latter drug. According to the literature (Lyng et al., 1991), it could be suggested that, although MX is inserted perpendicularly to the base-pair longest dimension, anthrapyrazoles are oriented more parallel to it.

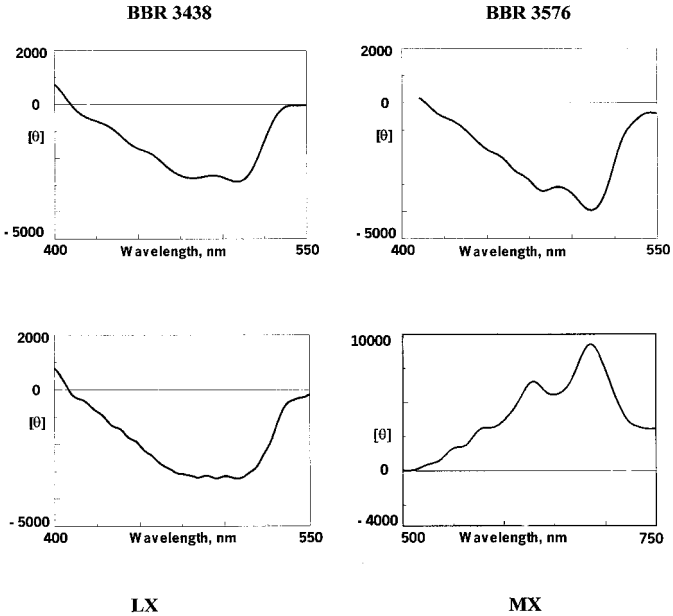

Fig. 7. Circular dichroism induced in the visible region by the binding of the test drugs to poly(dG-dC). DNA base to drug ratios were on the order of 25.

Differences in pharmacophore orientation and loss of hydroxy functions in the planar portion of the test drugs could explain the remarkably reduced topoisomerase poisoning effects found for 9-aza-APs. In fact, the less hydroxylated LX is remarkably less effective than MX in stimulating topoisomerase II-mediated drug-stimulated DNA cleavage. Moreover, introduction of the extra ring in LX also seems to reduce stimulation effects. The loss of rotational freedom in one of the side-chains probably prevents the drug from adjusting properly at the interface of the enzyme-DNA cleavage complex. Finally, protein-mediated DNA breaks are minimized when the extra nitrogen is introduced in the planar system, as in the 9-aza-APs. In line with the present findings, enzyme-mediated DNA damage was largely suppressed when the C-N bioisosteric substitution was introduced in the anthracenedione family (De Isabella et al., 1995).

These data, along with the fact that drug stimulation of enzyme-mediated cleavage exhibits very similar sequence specificity for all tested compounds, suggest that the prominent biological activity exhibited by the 9-aza-APs cannot be primarily explained, both qualitatively and quantitatively, in terms of topoisomerase II poisoning. Hence, a major cell-killing role should be played by other, non topoisomerase mediated, mechanism(s) (e.g., redox cycling) operating in this class of compounds.

Finally, 9-aza-APs exhibit (in the neutral state) an increased hydrophobicity compared with MX and LX. This renders them more likely to cross biological membranes and reach the intracellular target(s). Indeed, cell uptake measurements show that BBR 3438 reaches intracellular concentrations remarkably higher than LX (R. Supino, personal communication).

In conclusion, our studies demonstrate that 9-aza-APs exhibit physicochemical and DNA-binding properties that are well-distinct from their carbocyclic analogs. These could account for the promising preclinical profile, which renders them very interesting new leads for the development of effective anticancer drugs.

References

Arcamone FM (1998) From the pigments of the actinomycetes to third generation antitumor anthracyclines. *Biochimie* **80:**201–206.
Beylin VG, Colbry NL, Goel OP, Haky JE, Johnson DR, Kanter GD, Leeds RL, Leja B, Lewis EP, Rithner CD, Showalter HDH, Sercel AD, Turner WR and Uhlendorf SE (1989) Anticancer anthrapyrazoles. Improved synthesis of clinical agent CI-937, CI-941, and piroxantrone hydrochloride. *J Heterocycl Chem* **26:**85–96.
De Isabella P, Palumbo M, Sissi C, Capranico G, Carenini N, Menta E, Oliva A, Spinelli S, Krapcho AP, Giuliani FC and Zunino F (1995) Topoisomerase II DNA cleavage stimulation, DNA binding activity, cytotoxicity and physico-chemical properties of 2-aza- and 2-aza-oxide-anthracenedione derivatives. *Mol Pharmacol* **48:**30–38.
De Isabella P, Palumbo M, Sissi C, Carenini N, Capranico G, Menta E, Oliva A, Spinelli S, Krapcho AP, Giuliani FC and Zunino F (1997) Physicochemical properties, cytotoxic activity and topoisomerase II inhibition of 2,3-diaza-anthracenediones. *Biochem Pharmacol* **53:**161–169.
Denny WA and Wakelin LP (1990) Kinetics of the binding of mitoxantrone, ametantrone and analogues to DNA: Relationship with binding mode and anti-tumour activity. *Anti-Cancer Drug Des* **5:**189–200.
Frishman WH, Sung HM, Yee HC, Liu LL, Keefe D, Einzig AI and Dutcher J (1997) Cardiovascular toxicity with cancer chemotherapy. *Curr Probl Cancer* **21:**301–360.
Giantris A, Abdurrahman L, Hinkle A, Asselin B and Lipshultz SE (1998) Anthracycline-induced cardiotoxicity in children and young adults. *Crit Rev Oncol Hematol* **27:**53–68.
Grant RC, Harwood SJ and Wells RD (1968) The synthesis and characterization of poly d(I-C)·poly d(I-C). *J Am Chem Soc* **90:**4474–4476.
Halgren TA (1996a) Merck molecular force field. III. Molecular geometries and vibrational frequencies for MMFF94. *J Comput Chem* **17:**553–586.
Halgren TA (1996b) Merck molecular force field. IV. Conformational energies and geometries for MMFF94. *J Comput Chem* **17:**587–615.

Halgren TA (1996c) Merk molecular force field. I. Basis, form, scope, parameterization and performance of MMFF94. *J Comput Chem* **17:**490–519.
Halgren TA and Nachbar R (1996) Merck molecular force field. V. Extension of MMFF94 using experimental data, additional computational data, and empirical rules. *J Comput Chem* **17:**616–632.
Hartley JA, Reszka K, Zuo ET, Wilson WD, Morgan AR and Lown JW (1988) Characteristics of the interaction of anthrapyrazole anticancer agents with deoxyribonucleic acids: Structural requirements for DNA binding, intercalation, and photosensitization. *Mol Pharmacol* **33:**265–271.
Hazlehurst LA, Krapcho AP and Hacker MP (1995a) Comparison of aza-anthracenedione-induced DNA damage and cytotoxicity in experimental tumor cells. *Biochem Pharmacol* **50:**1087–1094.
Hazlehurst LA, Krapcho AP and Hacker MP (1995b) Correlation of DNA reactivity and cytotoxicity of a new class of anticancer agents: Aza-anthracenediones. *Cancer Lett* **91:**115–124.
Hortobagyi GN (1997) Anthracyclines in the treatment of cancer. An overview. *Drugs* **54(Suppl 4):**1–7.
Krapcho AP, Petry ME, Getahun Z, Landi JJ Jr, Stallman J, Polsenberg JF, Gallagher CE, Maresch MJ, Hacker MP, Giuliani FC, Beggiolin G, Pezzoni G, Menta E, Manzotti C, Oliva A, Spinelli S and Tognella S (1994) 6,9-Bis[(aminoalkyl)amino]benzo[g]isoquinoline-5,10-diones. A novel class of chromophore-modified antitumor anthracene-9,10-diones: Synthesis and antitumor evaluations. *J Med Chem* **37:**828–873.
Krapcho AP, Maresch MJ, Hacker MP, Hazelhurst L, Menta E, Oliva A, Spinelli S, Beggiolin G, Giuliani FC, Pezzoni G and Tognella S (1995) Anthracene-9,10-diones and aza-bioisosteres as antitumor agents. *Curr Med Chem* **2:**803–824.
Krapcho AP and Menta E (1997) Antitumor Aza-anthrapyrazoles. *Drugs Future* **22:**641–646.
Krapcho AP, Menta E, Oliva A, Di Domenico R, Fiocchi L, Maresch E, Gallagher CE, Hacker MP, Beggiolin G, Giuliani FC, pezzoni G and Spinelli S (1998) Synthesis and antitumor evaluation of 2,5-disubstituted-indazolo[4,3-gh]isoquinoline-6(2H)-ones (9-aza-anthrapyrazoles). *J Med Chem* **41:**5429–5444.
Lown JW, Morgan AR, Yen SF, Wang YT and Wilson WD (1985) Characteristics of the binding of the anticancer agents mitoxantrone and ametantrone and related structures to deoxyribonucleic acids. *Biochemistry* **24:**4028–4035.
Lyng R, Rodger A and Norden B (1991) The CD of ligand-DNA systems. I. Poly(dG-dC) B-DNA. *Biopolymers* **31:**1709–1720.
Malonne H and Atassi G (1997) DNA topoisomerase targeting drugs: Mechanisms of action and perspectives. *Anticancer Drugs* **8:**811–822.
Maxam AH and Gilbert W (1977) A new method for sequencing DNA. *Proc Natl Acad Sci USA* **74:**560–564.
McGhee JD and Von Hippel PH (1974) Theoretical aspects of DNA-protein interactions. Cooperative and non cooperative binding of large ligands to a one-dimensional homogeneous lattice. *J Mol Biol* **86:**469–489.
Perry PJ, Gowan SM, Reszka AP, Polucci P, Jenkins TC, Kelland LR and Neidle S (1998) 1,4- and 2,6-disubstituted amidoanthracene-9,10-dione derivatives as inhibitors of human telomerase. *J Med Chem* **41:**3253–3260.
Perry PJ, Read MA, Davies RT, Gowan SM, Reszka AP, Wood AA, Kelland LR and Neidle S (1999) 2,7-Disubstituted amidofluorenone derivatives as inhibitors of human telomerase. *J Med Chem* **42:**2679–2684.
Powis G and Kovach JS (1983) Disposition of bisantrene in humans and rabbits: Evidence for intravascular deposition of drug as a cause of phlebitis. *Cancer Res* **43:**925–929.
Record MT Jr, Anderson CF and Lohman TM (1978) Thermodynamic analysis of ion effects on the binding and conformational equilibria of proteins and nucleic acids: The roles of ion association on release, screening, and ion effects on water activity. *Q Rev Biophys* **11:**103–178.
Showalter HDH, Johnson JL, Hoftiezer JM, Turner WR, Werbel LM, Leopold WR, Shillis JL, Jackson RC and Elslager EF (1987) Anthrapyrazole anticancer agents. Synthesis and structure-activity relationship against murine leukemias. *J Med Chem* **30**:121–131.
Sissi C, Capranico G, Menta E and Palumbo M (1996) Aza-bioisosteres of 9,10-anthracenedione: A modulation of DNA sequence specificity. *Mol Pharmacol* **50:**838–845.
Sissi C, Moro S, Krapcho AP, Menta E and Palumbo M (1999) Binding of 2-aza-anthracenedione regioisomers to DNA: Effects of the relative position of side chain groups. *Anti-Cancer Drug Des* **14:**265–274.
Talbot DC, Smith IE, Mansi JL, Hudson I, Calvert AH and Ashley SE (1991) Anthrapyrazole CI-941: A highly active new agent in the treatment of advanced breast cancer. *J Clin Oncol* **9:**2141–2147.
Thomas X and Archimbaud E (1997) Mitoxantrone in the treatment of acute myelogenous leukemia: A review. *Hematol Cell Ther* **39:**63–74.
Walsh SM, Walley WM, Chandra M, Huan SD, Veinot JP and Higginson LAJ (1995) Potential cardiotoxicity with the use of DuP-941: A case report. *Can J Cardiol* **11:**419–422.
Wells RD, Larson JE, Grant RC, Shortle BE and Cantor CR (1970) Physicochemical studies on polydeoxyribonucleotides containing defined repeating nucleotide sequences. *J Mol Biol* **54:**465–497.
Wiseman LR and Spencer CM (1997) Mitoxantrone. A review of its pharmacology and clinical efficacy in the management of hormone-resistant advanced prostate cancer. *Drugs Aging* **10:**473–485.

Send reprint requests to: Manlio Palumbo, Dept. of Pharmaceutical Sciences, University of Padova, via Marzolo 5, 35131 Padova, Italy. E-mail: mpalumbo@purple.dsfarm.unipd.it